

# Brief Communication: The reliability of gas extraction techniques for analysing CH<sub>4</sub> and N<sub>2</sub>O compositions in gas trapped in permafrost ice-wedges

Ji-Woong Yang<sup>1\*</sup>, Jinho Ahn<sup>1</sup>, Go Iwahana<sup>2</sup>, Sangyoung Han<sup>1</sup>, Kyungmin Kim<sup>1\*\*</sup> and Alexander Fedorov<sup>3,4</sup>

<sup>1</sup>School of Earth and Environmental Sciences, Seoul National University, Seoul, South Korea

<sup>2</sup>International Arctic Research Center, University of Alaska, Fairbanks, USA

<sup>3</sup>Melnikov Permafrost Institute, Russian Academy of Science, Yakutsk, Russia

<sup>4</sup>North-Eastern Federal University, Yakutsk, Russia

\*Now at: Laboratoire des Sciences du Climat et de l'Environnement, LSCE/IPSL, CEA-CNRS-UVSQ, Université Paris-Saclay, Gif-sur-Yvette, France

\*\*Now at: Division of Earth and Planetary Materials Science, Department of Earth Science, Graduate School of Science, Tohoku University, Sendai, Japan

**Correspondence:** Jinho Ahn ([jinhoahn@snu.ac.kr](mailto:jinhoahn@snu.ac.kr))

**Abstract.** Methane (CH<sub>4</sub>) and nitrous oxide (N<sub>2</sub>O) compositions in ground ice may provide information on their production mechanisms in permafrost. However, existing gas extraction methods has not been well tested. We test conventional wet and dry gas extraction methods using ice-wedges from Alaska and Siberia. We find that both methods extract gas from the easily extractable parts of the ice (e.g., gas bubbles), and yield similar results for CH<sub>4</sub> and N<sub>2</sub>O mixing ratios. We also find insignificant effects of microbial activity during wet extraction. However, both techniques are unable to fully extract gas from the ice, presumably because gas molecules adsorbed onto or enclosed in soil aggregates are not easily extractable. Estimation of gas production in subfreezing environment of permafrost should consider the incomplete gas extraction.

## 1. Introduction

Permafrost preserves large amounts of soil carbon (C) and nitrogen (N) in a frozen state

30 (e.g., Hugelius et al., 2014; Salmon et al., 2018), temporarily removing this frozen carbon and  
31 nitrogen from active global cycles. Therefore, future projections of permafrost stability are of  
32 great interest, particularly because thawing permafrost may lead to decomposition and/or  
33 remineralization of the buried soil C and N and their abrupt emission into the atmosphere in  
34 the form of greenhouse gases (GHGs) – carbon dioxide (CO<sub>2</sub>), methane (CH<sub>4</sub>), and nitrous  
35 oxide (N<sub>2</sub>O), which in turn can trigger positive feedbacks (e.g., Salmon et al., 2018). In addition,  
36 the projected polar amplification (e.g., Masson-Delmotte et al., 2013) may strengthen these  
37 positive feedbacks. However, the processes responsible for in-situ C and N remineralization  
38 and GHG production in ground ice are poorly understood, despite the fact that ground ice  
39 accounts for a substantial portion (up to approximately 40–90% by volume) of Pleistocene ice-  
40 rich permafrost, or Yedoma (e.g., Kanevskiy et al., 2013; Jorgenson et al., 2015).

41         The gases trapped in ground ice allow unique insights into the origin of ground ice and  
42 evidence for in-situ microbial aerobic and anaerobic respirations (Boereboom et al., 2013; Kim  
43 et al., 2019; Lacelle et al., 2011). Among others, the GHGs in ground ice may provide detailed  
44 information on in-situ biogeochemical processes responsible for GHG production (i.e.,  
45 methanogenesis, nitrification, and denitrification) (e.g., Boereboom et al., 2013; Kim et al.,  
46 2019). However, analytical methods remain poorly scrutinized. Boereboom et al. (2013)  
47 utilized the conventional melting-refreezing method (wet extraction) used in polar ice core  
48 analyses. In this technique, the ice samples were melted under a vacuum to liberate the enclosed  
49 gases, then refrozen to expel the dissolved gases present in the meltwater. Other studies  
50 conducted by Russian scientists used an on-site melting method in which a large (1–3 kg) block  
51 of ground ice sample was melted in a saturated sodium chloride (NaCl) solution, in order to  
52 minimize gas dissolution (Arkhangelov and Novgorodova, 1991). A recent study instead used  
53 a dry extraction technique to prevent the microbial activity during wet extraction (Kim et al.,  
54 2019), which employed a needle-crusher in a vacuum to crush approximately 10 g of ice sample

55 without melting (Shin, 2014).

56 In this study, for the first time we test the reliability of both wet and dry extraction  
57 methods for CH<sub>4</sub> and N<sub>2</sub>O mixing ratios and contents (volume or moles of gas in a unit mass  
58 at standard temperature and pressure conditions (STP)) using permafrost ground ice samples.  
59 Ice-wedge samples from Alaskan and Siberian permafrost were used because ice wedges are  
60 one of the most abundant morphological features of massive ground ice, consisting of  
61 approximately 5 to 50% by volume of the upper permafrost (Kanevskiy et al., 2013; Jorgenson  
62 et al., 2015). More specifically, this study aims to address the following scientific questions: 1)  
63 Do wet and dry extraction methods yield different results? 2) Are the melting-refreezing results  
64 affected by microbial activity during gas extraction? 3) How effectively does the wet/dry  
65 extraction extract gases from ice wedges? To address the first question, CH<sub>4</sub> and N<sub>2</sub>O results  
66 from dry and wet extractions were compared. For the second question, we applied the wet  
67 extraction method to both biocide-treated and control samples. Finally, for the third question  
68 we carried out tests with and without extended number of hitting ice with a needle system in a  
69 crushing chamber, as well as additional dry extraction from ice samples that had been degassed  
70 by our wet extraction method.

71

## 72 **2. Materials and Methods**

### 73 **2.1. Ice samples and sample preparation**

74 The ice-wedge samples used in this study were collected from Churapcha, Cyuie  
75 (central Yakutia), and Zyryanka (north-eastern Yakutia) in Siberia, as well as from northern  
76 Alaska (Supplementary Figure 1). The Churapcha site (61.97°N, 132.61°E) is located  
77 approximately 180 km east of Yakutsk. The Cyuie site (61.73°N, 130.42°E) is located  
78 approximately 30 km southeast of Yakutsk. The Cyuie samples were collected from two  
79 outcrops (CYB and CYC) (Kim et al., 2019). At each site, 30 cm long ice-wedge cores were

80 drilled perpendicular to the outcrop surface (Supplementary Figures 2 and 3).

81 Zyryanka is located in the southern boreal region of the Kolyma River, at the junction  
82 of the Chersky and Yukaghir Ranges, in a region affected by thermokarst development  
83 (Fedorov et al., 1991). Site A (Zy-A) is located on a tributary of the Kolyma River,  
84 approximately 22 km north of Zyryanka. Site B (Zy-B) is approximately 14 km west of the  
85 start of the Kolyma tributary, which begins ~11 km north of Zyryanka. Site F (Zy-F) is located  
86 approximately 4 km west of the tributary that leads to site B. The ground ice samples were  
87 collected from riverbank walls exposed by lateral erosion using a chainsaw (Supplementary  
88 Figure 4). Most of the outcrops that were sampled for ground ice were on the first (lowest)  
89 terrace of the river.

90 For the Alaskan sampling locations, Bluff03 (69.40°N, 150.95°W) and Bluff06  
91 (69.14°N, 150.61°W) are located in the Alaska North Slope region, approximately 120 and 150  
92 km from the Arctic Ocean, or 100 and 70 km northwest of the Toolik Field Station (68.63°N,  
93 149.59°W), respectively. Samples from Bluff03 were collected from the bluff walls that had  
94 developed by gully formations on a gentle slope of the Yedoma using a chainsaw. Samples of  
95 Bluff06 were collected from outcrops within eroded frozen peatland in a thaw lake basin  
96 (Supplementary Figure 5). All the ice-wedge samples used in this study were stored in a chest  
97 freezer at  $< -18^{\circ}\text{C}$  before analysis.

98 The ice-wedge ice is most different from polar ice cores, in that their gas mixing ratios  
99 are not homogeneous (e.g., Kim et al., 2019), which may hinder exact comparison with results  
100 from adjacent ice samples. We therefore randomly mixed sub-samples to reduce the effect of  
101 the heterogeneous gas composition distribution (random cube method hereafter).  
102 Approximately 100–200 g of an ice-wedge sample was cut into 25 to 50 cubes of 3–4 g each,  
103 and for each experiment, ~10 to 12 cubes were randomly chosen so that the total weight of the  
104 sub-sample was ~40 g.

105 **2.2. Gas extraction procedures**

106 ***Dry extraction (needle crusher)***

107 For dry extraction, we used a needle-crusher system at the Seoul National University  
108 (SNU, Seoul, South Korea) (Shin, 2014). In brief, 8~13 g of ice sample were crushed in a cold  
109 vacuum chamber (extraction chamber). The ice samples were usually hit five times by the  
110 needle set. The temperature within the extraction chamber was maintained at -37°C by using a  
111 cold ethanol-circulating chiller. The extracted gas was dried by passing it through a water vapor  
112 trap at -85°C and cryogenically trapping it in a stainless-steel tube (sample tube) at  
113 approximately -257 °C using a helium closed-cycle refrigerator (He-CCR). Since the extraction  
114 chamber cannot accommodate ~40 g of ice at once, the ~40 g of random cube sub-samples  
115 were extracted using three sequential extractions and the gas liberated from each extraction  
116 was trapped in a sample tube.

117 Following extraction, the sample tubes were detached from the He-CCR, warmed to  
118 room temperature (~20°C), and attached to a gas chromatograph (GC) equipped with an  
119 electron capture detector (ECD) and a flame ionization detector (FID) to determine the mixing  
120 ratios of CH<sub>4</sub> and N<sub>2</sub>O. Details of the GC system are given in Ryu et al. (2018). The daily  
121 calibration curves were established using working standards of 15.6 ± 0.2 ppm CH<sub>4</sub>, 10000 ±  
122 30 ppm CH<sub>4</sub>, 2960 ± 89 ppb N<sub>2</sub>O, 29600 ± 888 ppb N<sub>2</sub>O, and a modern air sample from a  
123 surface firn at Styx Glacier, Antarctica (obtained in November 2016), which was calibrated as  
124 1758.6 ± 0.6 ppb CH<sub>4</sub> and 324.7 ± 0.3 ppb N<sub>2</sub>O by the National Oceanic and Atmospheric  
125 Administration (NOAA).

126

127 ***Wet extraction (melt-refreeze)***

128 For the control and HgCl<sub>2</sub>-treated wet extraction experiments, a melting-refreezing wet  
129 extraction system at SNU was employed (Yang et al., 2017; Ryu et al., 2018). The gas

130 extraction procedure is identical to the procedure described in Yang et al. (2017) and Ryu et al.  
131 (2018), except for the sample gas trapping procedure (see below). Ice-wedge sub-samples of  
132 ~40 g (composed of 10–12 ice cubes for each) were placed in a glass container welded to a  
133 stainless-steel flange (sample flask), and the laboratory air inside the sample flasks was  
134 evacuated for 40 min. The sample flasks were then submerged in a warm (~50°C) tap water  
135 bath to melt the ice samples. After melting was complete, the meltwater was refrozen by  
136 chilling the sample flasks with cold ethanol (below -70°C). The sample gas in the headspace  
137 of each sample flask was then expanded to the volume-calibrated vacuum line to estimate the  
138 volume of extracted gas, and trapped in a stainless-steel sample tube by the He-CCR device.  
139 In this study, we attached the He-CCR device to our wet extraction line and the gas samples in  
140 the flasks were cryogenically trapped. The reasons for using He-CCR instead of direct  
141 expansion to a GC are twofold: 1) to better compare the dry and wet extraction methods by  
142 applying the same trapping procedure, and 2) to maximize the amount of sample gas for GC  
143 analysis, because the gas expansion from a large flask allows only a small fraction of gas to be  
144 measured by the GC.

145 For biocide-treated tests, 1.84 mmol of mercuric chloride ( $\text{HgCl}_2$ ) was applied per unit  
146 kilogram of soil, following established procedures for soil sterilization (Fletcher and Kaufman,  
147 1980). We obtained the average dry soil mass (0.33 g) from the leftover meltwater samples of  
148 the previous wet extractions, which were carried out for comparison between dry- and wet  
149 extractions. Taking the average dry soil mass (0.33 g) into account, we added 24  $\mu\text{L}$  of saturated  
150  $\text{HgCl}_2$  solution (at 20°C) to the sample flasks. The flasks with  $\text{HgCl}_2$  solution were then frozen  
151 in a deep freezer at  $< -45^\circ\text{C}$  to prevent the dissolution of ambient air into the solution during  
152 ice sample loading. After the wet extraction procedure was complete, the extracted gas was  
153 trapped in a sample tube and the  $\text{CH}_4$  and  $\text{N}_2\text{O}$  mixing ratios were determined using the same  
154 GC-ECD-FID system as the dry-extracted gas. The resulting  $\text{CH}_4$  and  $\text{N}_2\text{O}$  mixing ratios have

155 not been corrected for partial dissolution in ice melt in the flasks, because CH<sub>4</sub> and N<sub>2</sub>O trapped  
156 in refrozen ice are negligible compared to the ranges of the systematic blanks (see Appendix).

157

### 158 **2.3. Gas content**

159 The analytical methods described previously are for determining the mixing ratios of  
160 CH<sub>4</sub> and N<sub>2</sub>O in the extracted gas. To convert these mixing ratios into moles of CH<sub>4</sub> and N<sub>2</sub>O  
161 per unit mass of ice-wedge sample (CH<sub>4</sub> and N<sub>2</sub>O content, respectively, hereafter) requires data  
162 regarding the amount of gas extracted. The gas content is a measure of gas volume enclosed in  
163 a unit mass of ice sample at STP (in mL kg<sub>ice</sub><sup>-1</sup>). Thus, the CH<sub>4</sub> and N<sub>2</sub>O contents can be  
164 calculated using the gas content, the total mass of the random cube ice, and the gas mixing  
165 ratio. The gas content in the control and HgCl<sub>2</sub>-treated wet extraction experiments was  
166 calculated from the temperature and pressure of the extracted gas and the internal volume of  
167 the vacuum line. The details of the extraction system and correction methods used for  
168 estimating gas content are described in Yang (2019). Similarly, the gas content of the dry  
169 extraction samples was also inferred from the volume and pressure of gas inside the vacuum  
170 line once the sample tube was attached to the line for GC analysis. The uncertainties of the  
171 calculated CH<sub>4</sub> and N<sub>2</sub>O contents were calculated by using error propagation of the blanks and  
172 gas content uncertainties (see Appendix for uncertainty estimation of the blank corrections and  
173 gas contents).

174

### 175 **2.4. Dry soil content**

176 Dry soil content was measured using the leftover meltwater from the control-wet  
177 extraction tests. After the control-wet extractions were complete, the sample flasks were shaken  
178 thoroughly and the meltwater samples were each poured into a 50 mL conical tube. The  
179 meltwater and soils were separated by a centrifugal separator at 3000 rpm for 10 min. The

180 separated wet soils were wind-dried in evaporating dishes at approximately 100°C for 24 hours.  
181 The weight of each individual evaporating dish was pre-measured before use. The dry soil  
182 content was calculated by subtracting the weight of the evaporating dish from the total weight  
183 of the dried soil sample plus the evaporating dish.

184

### 185 **3. Results and Discussion**

#### 186 **3.1. Comparison between wet and dry extraction methods**

187 The results from the wet and dry extractions were compared using 23 ice-wedge  
188 samples (21 for N<sub>2</sub>O) from Alaska and Siberia. In both the CH<sub>4</sub> and N<sub>2</sub>O mixing ratio analyses,  
189 we found that the wet and dry extraction results did not differ significantly ( $p > 0.1$ ), regardless  
190 of sampling site or soil content (Figure 1, a to d). We note that the heterogeneous distribution  
191 of gas mixing ratios of in centimetre scales (Kim et al., 2019) may not have been completely  
192 smoothed out by our sub-sample selection, although we randomly chose 8–12 ice cubes for  
193 each measurement. Some previous studies have avoided using the wet extraction method  
194 because of potential reactivation of microbial CH<sub>4</sub> and/or N<sub>2</sub>O production in ice melt (e.g.,  
195 Cherbunina et al., 2018; Kim et al., 2019). Assuming that activation of microbial metabolism  
196 is unlikely during dry extraction at a temperature of -37°C in the extraction chamber for < 1 h,  
197 our findings may imply that wet extraction does not stimulate microbial reactivation to a  
198 measurable extent.



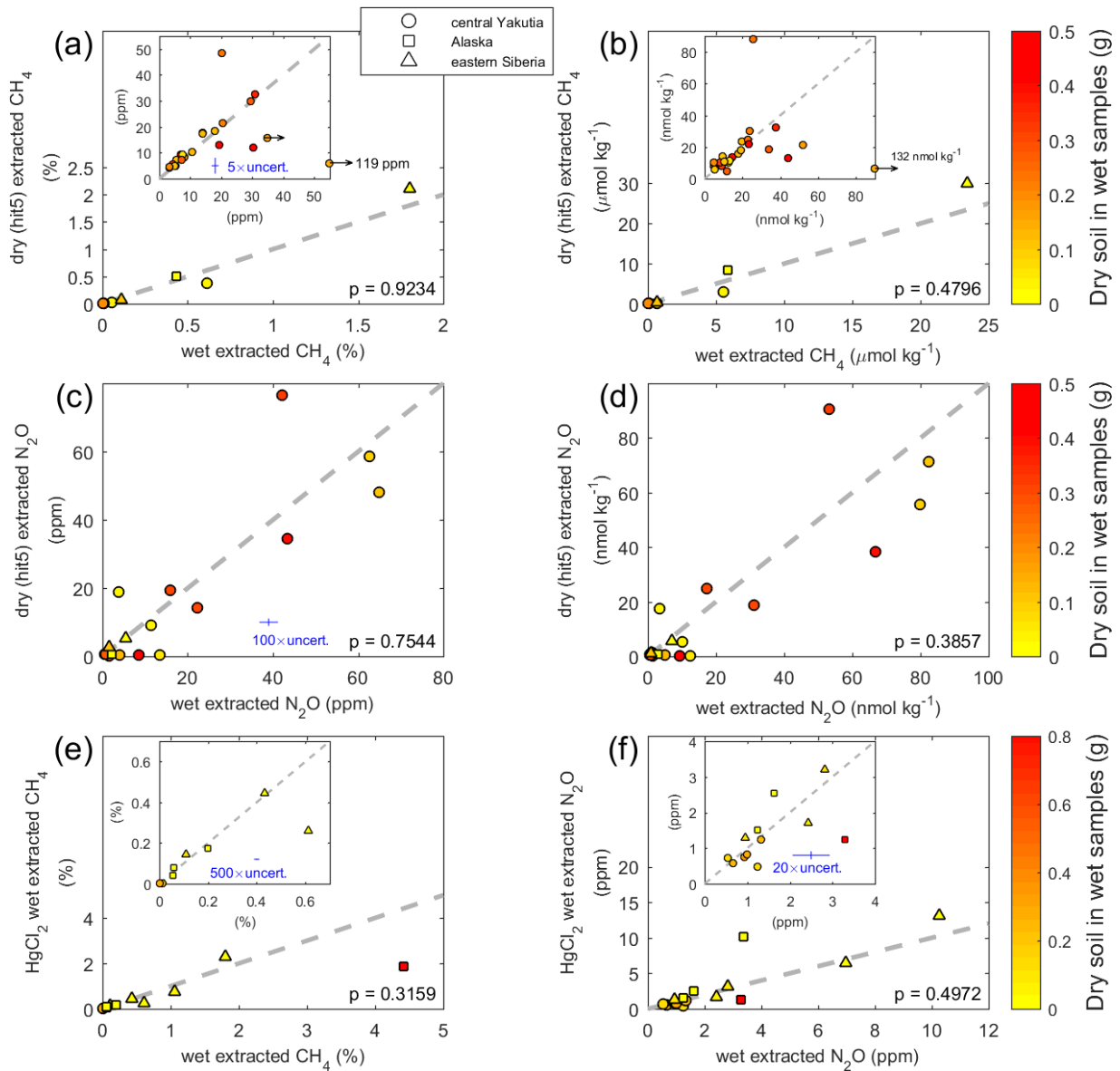


**Figure 1.** Comparison of CH<sub>4</sub> and N<sub>2</sub>O mixing ratios and contents obtained by different extraction methods. Shown are scatter plots between wet- and dry (hit5) extraction results of CH<sub>4</sub> (a and b) and N<sub>2</sub>O (c and d), and between control- and biocide-treated wet extraction results for CH<sub>4</sub> (e) and N<sub>2</sub>O (f). The ‘hit5’ denotes the dry extraction with five times hitting (see Section 3.3). Left panels (a, c, and e) and (f) present in mixing ratios of gas in bubbles, while right (b) and (d) panels in moles of gas in a unit mass of ice (gas content). The sampling locations are indicated by different symbols. The color of each data point indicates the dry soil weight in the subsamples used in control wet extraction. The 1-sigma uncertainties of the mixing ratios (a, c, e, and f) are magnified by 5x, 20x, 100x, and 500x as denoted as blue error bars (see Appendix). The error bars are not visible where the error bars are smaller than markers. The grey dashed lines are 1:1 reference line. Note that the units of the axes of the insets in (e) and (f) are identical to the original plots. The p-value of two-sided Students’ t-test of each comparison is denoted at the bottom right corner of each plot.

199

200

### 201 **3.2. Testing microbial alteration during wet extraction**

202 To test the microbial production of CH<sub>4</sub> and N<sub>2</sub>O during wet extraction more accurately,  
203 we conducted wet extraction experiments on samples treated with HgCl<sub>2</sub>, a commonly used  
204 effective biocide (e.g., Torres et al., 2005), and compared the results with those of untreated  
205 (control) wet extractions. We prepared 12 additional ice-wedge samples using the random cube  
206 method for these tests (see Materials and Methods section). We found no significant differences  
207 between the control and HgCl<sub>2</sub>-treated wet extraction results for both CH<sub>4</sub> and N<sub>2</sub>O mixing  
208 ratios (Figures 1e and 1f), indicating that the bias due to microbial activity during  
209 approximately an hour of the melting-refreezing procedure is not significant. This is further  
210 supported by tests on an additional 12 ice-wedge samples (using the random cube protocol)  
211 treated with 2-bromo-ethane-sulfonate (BES), a specific methanogenesis inhibitor (e.g., Nollet  
212 et al., 1997) (Figure A3). Similar to the HgCl<sub>2</sub>-treated experiments, 25 μL of a saturated BES  
213 solution was added to each sample flask. These additional tests were carried out only for CH<sub>4</sub>.  
214 The two-sided t-test for the CH<sub>4</sub> data indicates an insignificant difference between the two  
215 results ( $p > 0.9$ ). Data from individual sampling sites also do not show significant differences  
216 ( $p > 0.9$  for the Alaskan samples and  $p > 0.5$  for the central Yakutian samples).

217 According to microbial sequencing studies that have shown the presence of viable  
218 microbes in permafrost and ground ice (e.g., Katayama et al., 2007), it is likely that culturable  
219 microbes exist in the ice-wedge samples used in this study. However, considering that at least  
220 14 days and up to 3 months of culturing was required to identify microbe colonies extracted  
221 from ground ice (Katayama et al., 2007; Lacelle et al., 2011), our melt-refreeze time of an hour  
222 was insufficient for microbial activity to resume and produce CH<sub>4</sub> and N<sub>2</sub>O.

223

### 224 **3.3. Dry extraction efficiency and gas mixing ratios**

225 One limitation of our needle crushing dry-extraction technique is the inability to

226 completely extract gas from ice samples, because small ice particles and/or flakes placed in the  
227 space between the needles are not fully crushed. The gas extraction efficiency of the SNU  
228 needle crusher system has been reported as ~80–90% for polar ice core samples (Shin, 2014).  
229 However, the gas extraction efficiency has not been tested for ice-wedge samples. Depending  
230 on the extraction efficiency, the needle crushing method could underestimate the gas contents  
231 if the gas is not completely extracted. Another possible bias in the gas mixing ratios arises if  
232 the CH<sub>4</sub> and N<sub>2</sub>O compositions are different between the crushed and uncrushed portions of  
233 the ice-wedge samples.

234 To estimate the biases arising from incomplete gas extraction, we designed a series of  
235 tests to identify the differences of the CH<sub>4</sub> and N<sub>2</sub>O mixing ratios and contents between the  
236 crushed and uncrushed sample portions. Each ice-wedge sample that was randomly collected  
237 was first crushed by the regular dry extraction procedure (by hitting it five times with the needle  
238 system, ‘hit5’), and the gas liberated from the sample was trapped in a sample tube. Then we  
239 performed an additional 100 hits on the leftover ice (‘hit100’), monitored the amount of  
240 additional gas liberated, and trapped the additional gas in a separate sample tube. Comparisons  
241 between the hit5 and hit100 results are summarized in Table 1.

242 Here we regard the ratio of gas content of hit100 to that of hit5 (hit100/hit5 ratio  
243 hereafter) as a measure of the gas extraction efficiency of the needle crusher system. The results  
244 demonstrate an average hit100/hit5 ratio of gas content of  $0.40 \pm 0.07$  for the Zyryanka samples,  
245  $0.24 \pm 0.07$  for the Bluff samples, and  $0.14 \pm 0.11$  for the Cyuie samples (Table 1). Despite the  
246 fact that the number of samples was limited, the ice-wedge samples from the different sites  
247 show distinct hit100/hit5 ratios of the amount of extracted gas. However, we observed that the  
248 leftover ice from the Bluff and Zyryanka samples were not well-crushed, even after 100 hits  
249 with the needle crusher. This was especially true if the ice sub-samples contained soil  
250 aggregates: the frozen soil aggregates were barely crushed. In contrast, the Cyuie samples were

251 relatively well-crushed, and the leftover samples were apparently finer-sized ice flakes. We  
252 also observed that the hit100/hit5 ratios of gas content are highly variable within samples from  
253 a particular site, implying that the extraction efficiency of the needle crusher not only depends  
254 on site characteristics, but also on the individual ice sample hardness. When compared with the  
255 dry soil content measured from the sub-samples used for wet extraction, no relationship was  
256 observed between the dry soil content and the extraction efficiency (Figures 1 and A3). In  
257 addition, in the case of samples uncrushed by the hit100 test, it is difficult to estimate the  
258 extraction efficiency using the hit100/hit5 ratio of gas content, as the hit100 tests liberated only  
259 a marginal portion of gas from these samples. This is because the large-sized uncrushed soil  
260 aggregates or particles may have prohibited the needle crusher from crushing the small-sized  
261 ice flakes or grains. The needles move up and down together, as they are fixed to a pneumatic  
262 linear motion feedthrough device, thus if there is a sizable soil clod that cannot be crushed, it  
263 blocks the needle crusher from moving further down. Therefore, we do not recommend using  
264 a needle crusher system to measure gas contents in ice-wedge samples.

265         The hardness of the ice samples may also affect the gas mixing ratio analysis in the hit5  
266 and hit100 procedures. The hit100/hit5 ratio of CH<sub>4</sub> mixing ratio of Bluff and Zyryanka  
267 samples are less than 1 in four out of six samples, yielding an average of  $0.9 \pm 0.5$ . However,  
268 all five samples from the Cyuie ice-wedges have ratios greater than 1, with an average of  $4.7$   
269  $\pm 2.6$  (Table 1). The higher hit100/hit5 ratio of CH<sub>4</sub> mixing ratios of Cyuie samples indicates  
270 that the gases extracted via the hit100 procedure have higher CH<sub>4</sub> mixing ratios than the gases  
271 extracted via the hit5 procedure. Considering these results with those discussed previously, we  
272 speculate that there are three ways gas can be trapped in ice-wedge ice: enclosed in bubbles,  
273 adsorbed on soil particles, and entrapped in soil aggregates. The better-crushed leftover ice  
274 flakes in the Cyuie samples may have allowed most of the gas in bubbles and part of the CH<sub>4</sub>  
275 molecules adsorbed on soil particles and/or trapped in microsites within soil aggregates to be

276 liberated. Thus, the hit5 CH<sub>4</sub> mixing ratios of the Cyuie samples may more reflect the gas  
277 mixing ratios in bubbles, while the hit100 results reflect more of the contribution from gas  
278 adsorbed on soil and trapped within soil aggregates than the hit5 results because the ice sample  
279 containing larger-sized aggregates has greater hardness than those with smaller aggregates or  
280 fine particles. If this is the case for the Cyuie samples, we can infer that CH<sub>4</sub> is more  
281 concentrated in soil particles and in microsites within soil aggregates, compared to in bubbles  
282 in the ice. This is partly supported by evidence that ice-wedge layers exhibit relatively trace  
283 amounts of CH<sub>4</sub> compared to the surrounding permafrost soil layers (Rivkina et al., 2007);  
284 however, this needs to be further evaluated by detailed microbial and chemical analyses. In the  
285 meanwhile, in the Bluff and Zyryanka samples, the hit5 results reflect the mixing ratios of the  
286 gases from the crushed portions, regardless of their origin: bubbles, particle adsorption, or  
287 microsites in aggregates (Table 1). Given that some of the Bluff and Zyryanka ice-wedge  
288 samples were not fully crushed by the hit100 tests, it may require additional hits or another  
289 extraction technique. Unlike CH<sub>4</sub>, the N<sub>2</sub>O mixing ratios from the hit100 extractions are higher  
290 than the hit5 in ten out of eleven samples, regardless of the sampling site. The hit100/hit5 ratios  
291 of N<sub>2</sub>O mixing ratios of the Bluff and Zyryanka samples ( $1.9 \pm 0.8$  on average) are not  
292 significantly different ( $p = 0.32$ ) from those of the Cyuie samples ( $2.9 \pm 1.8$  on average). This  
293 can probably be explained by the fact that the N<sub>2</sub>O mixing ratio is not necessarily higher in  
294 soil-rich ice because N<sub>2</sub>O is an intermediate product of denitrification, while CH<sub>4</sub> is produced  
295 as the final product of methanogenesis.

296 One may expect that a different crushing technique might be more suitable for ice-  
297 wedge samples. However, none of the existing dry extraction techniques - centrifugal ice  
298 microtome (Bereiter et al., 2013), mechanical grater (Etheridge et al., 1988), or ball-mill  
299 crusher (Schaefer et al., 2011) is more advantageous for ice-wedge analysis compared to the  
300 needle crusher system used in this study. The hard portion of ice wedges (e.g., frozen soil

301 aggregates, large soil particles) could easily damage the metal blades of the centrifugal ice  
302 microtome and mechanical grater devices, or block the space within the ball-mill chamber,  
303 limiting the movement of the milling balls.

304         It is worth noting that friction between stainless steels could produce CH<sub>4</sub> with carbon  
305 from the damaged stainless-steel surface and hydrogen gas (Higaki et al., 2006). If needle  
306 crushing causes contamination in this way, the dry extraction results should be affected by the  
307 number of hits. To check the impact of the needle crushing procedure on ice-wedge CH<sub>4</sub> and  
308 N<sub>2</sub>O measurements, we carried out blank tests by changing the numbers of hits from 5 to 100.  
309 The results of these tests show no systematic offset among the experiments with different  
310 numbers of hits (Figure A2), which implies that the crushing procedure does not affect the dry  
311 extraction results for CH<sub>4</sub> and N<sub>2</sub>O. Even though a small of contamination does exist, its effects  
312 have already been subtracted via blank correction and taken into account in the overall error  
313 estimation (see Appendix). Therefore, we consider that our findings are not artefacts of metal  
314 friction during crushing.

315         To summarize, from the hit5 and hit100 comparison tests, we found that 1) the needle  
316 crusher method is not able to fully crush the ice-wedge ice samples and thus is unsuitable for  
317 measuring gas contents in a unit mass of ice, and that 2) weak crushing (e.g., a small number  
318 of hits by the needle crusher system) may better reflect gas mixing ratios of the soft parts of  
319 the samples (such as air bubbles) than strong crushing (e.g., a greater number of hits).

320 **Table 1.** Results of dry extraction tests with 5- and additional 100 times hitting ice-wedge samples, denoted as ‘hit5’ and ‘hit100’, respectively. ‘hit100/hit5’  
 321 is the ratio in extracted gas content or gas mixing ratio of ‘hit100’ to ‘hit5’ cases. Also shown are gas content results from both experiments, where the hit100  
 322 values are given both in the unit of ml kg<sup>-1</sup> at STP conditions and μmol/kg (in parenthesis). It should be noted that the ‘hit100’ gas content results indicate  
 323 the additional amount of gas extracted after ‘hit5’ crushing and evacuation.

Site Location	Sample	soil content	gas content				CH <sub>4</sub> mixing ratio				N <sub>2</sub> O mixing ratio			
			Wet control	Dry hit5	Dry hit100	hit100/hit5	Wet control	Dry hit5	Dry hit100	hit100/hit5	Wet control	Dry hit5	Dry hit100	hit100/hit5
		wt. %	ml/kg	ml/kg	ml/kg	ppm	ppm	ppm		ppm	ppm	ppm		
Zyryanka, Northeastern Siberia	Zy-A-W1-D	0.155	20.2	13.1	6.3	0.48	6138	3713	2721	0.7329	11.37	9.10	10.15	1.12
	Zy-F-1	0.618	13.5	8.1	3.4	0.42	1080	655.6	173.5	0.2646	1.57	2.81	2.65	0.942
	Zy-A-W1-Low	0.049	30.6	27.8	8.0	0.29	4309	5073	4818	0.9497	2.07	0.69	2.02	2.9
	Zy-B-Low-B	0.107	29.1	23.9	10.0	0.418	18030	21010	35290	1.680	5.37	5.32	15.36	2.89
Northern Alaska	Bluff03-IW1	2.07	13.2	12.2	2.6	0.21	44160	25230	12240	0.4851	5.58	2.36	4.93	2.09
	Bluff06-B3	0.078	20.1	20.9	5.6	0.27	558.7	164.2	219.5	1.337	3.74	18.78	30.14	1.605
Cyuié, Central Yakutia	CYC-01-B	0.252	18.0	21.7	7.1	0.33	18.0	18.3	25.4	1.39	1.55	1.60	2.59	1.62
	CYB-04-C	0.498	20.9	30.7	1.5	0.049	20.2	48.4	165.6	3.42	0.71	0.65	2.96	4.5
	CYB-03-A	0.420	19.7	23.7	1.0	0.041	20.5	21.5	67.1	3.12	0.91	1.01	1.06	1.05
	CYB-02-A	0.403	32.0	25.5	1.9	0.073	29.1	18.7	159.8	8.55	1.00	0.58	3.19	5.5
	CYC-03-B	0.830	22.6	15.7	3.3	0.21	20.3	13.9	94.5	6.80	1.40	0.65	1.08	1.7

### 324 **3.4. Residual gas mixing ratios and contents after wet extraction**

325 To examine how well the gas is extracted by wet extraction, we applied the dry  
326 extraction method to refrozen ice-wedge samples after wet extraction. We first prepared  
327 degassed ice-wedge samples that had undergone repetitive wet extractions (wet-degassed ice  
328 hereafter). Once the wet extraction experiments were completed, we repeated two cycles of  
329 melting-refreezing and evacuation procedures to degas the ice melt. After degassing by a total  
330 of three cycles of wet extraction and evacuation, the outermost surfaces (~2 mm) of the wet-  
331 degassed ice were trimmed away in the walk-in freezer at SNU on the morning of experiments.  
332 The wet-degassed ice was then inserted into the needle crusher and the crusher chamber was  
333 evacuated. A specific amount of standard air was injected. Then, the wet-degassed ice samples  
334 were hit 20 or 60 times by the needle crusher. The amount of gas and gas mixing ratio of the  
335 additionally extracted gas from the wet-degassed ice are shown in Figure 2 and Table A1.

336 The tests using the wet-degassed ice show an additional gas extraction of ~12 to 20 ml  
337  $\text{kg}_{\text{ice}}^{-1}$ , which is ~43 to 88% of the amount of gas extracted during the initial wet extraction.  
338 The additionally extracted gas from the dry extraction is referred to as residual gas hereafter.  
339 This is remarkably in contrast to the less than 1% residual fraction of the SNU wet extraction  
340 system for ice from polar ice sheets. If such a considerable amount of gas is left intact by  
341 repeated wet extractions, the composition of the additional gas is important to understand how  
342 much the conventional wet extraction results are biased.

343 Figure 2 and Table A1 show the mixing ratios and contents of  $\text{CH}_4$  and  $\text{N}_2\text{O}$  in the  
344 residual gas. The mixing ratios of the residual gas were estimated using mass balance  
345 calculations with observed mixing ratios and the amounts of the injected standard and extracted  
346 residual gas. The  $\text{CH}_4$  mixing ratios of the residual gas range from 10.37 to 23.78 ppm, which  
347 is similar to the range of the wet extracted gas. This evidence indicates that  $\text{CH}_4$  in ice-wedges  
348 cannot be fully extracted by a melting-refreezing procedure. We suspect two possible reasons



349 for this: (1) During wet extraction, the ice-wedge samples melted and the soil particles settled  
350 at the bottom of the sample flask without any physical impact to the soil particles, causing the  
351 adsorbed CH<sub>4</sub> molecules on the soil particles to remain adsorbed. (2) During refreezing, the  
352 soils accumulated at the bottom of the flasks are crumpled around the centre of the refrozen  
353 ice, because the sample flasks are chilled from outside, which facilitated gas entrapment within  
354 the frozen soil aggregate. In contrast, the N<sub>2</sub>O mixing ratios of the residual gas exhibit very  
355 low values compared to those from the initial wet extraction (Figure 2 and Table A1). These  
356 results imply that most of the N<sub>2</sub>O in ice wedges is extracted by three melting-refreezing cycles,  
357 such that only a small amount of N<sub>2</sub>O is left adsorbed or entrapped in ice-wedge soils. The  
358 authors posit that this might be attributed to the high solubility of N<sub>2</sub>O to water compared to  
359 CH<sub>4</sub>. However, it needs further investigation to better understand this.

360 In this section, we found that a certain amount of gas remained in ice wedges, even after  
361 three cycles of wet extraction, which is extractable instead by needle crushing. This implies  
362 that, unlike polar ice cores, wet extraction of ice-wedges does not guarantee near-complete gas  
363 extraction, and therefore, precise measurements of the gas content of ice wedges are difficult  
364 to obtain. The difficulty in measuring gas content imposes a large uncertainty in estimating  
365 CH<sub>4</sub> and N<sub>2</sub>O contents. Furthermore, we found that the residual gas has a similar order CH<sub>4</sub>  
366 mixing ratio as the gas extracted by initial melting-refreezing, indicating that a comparable  
367 amount of CH<sub>4</sub> still remains unextracted in ice-wedges. Hence, a novel extraction method is  
368 required to produce reliable gas content and gas mixing ratios in ice wedges. In contrast, our  
369 results show that the N<sub>2</sub>O content of the residual gas is at trace levels, which may suggest that  
370 most of the N<sub>2</sub>O in ice-wedges is extractable during initial melting-refreezing. Therefore, wet  
371 extraction could be applicable for estimating the N<sub>2</sub>O content of ice wedges. However, given  
372 that the above evidence resulted from three consecutive cycles of melting-refreezing and  
373 evacuation, it is unclear how many melting-refreezing cycles are required to extract most of

374 the N<sub>2</sub>O from ice wedges. It should be noted that combination of repetitive wet extractions with  
 375 dry extraction does not guarantee reliable estimation of N<sub>2</sub>O mixing ratio, because extraction  
 376 efficiency of the other gas components may be different from that of N<sub>2</sub>O. Our findings imply  
 377 that previous estimates of CH<sub>4</sub> budget in ground ice based on wet extraction principle (e.g.,  
 378 Boereboom et al., 2013; Cherbunina et al., 2018) might have been underestimated, and that the  
 379 CH<sub>4</sub> production within subfreezing permafrost environment could be larger than previously  
 380 estimated. Future study should be devoted to a novel extraction method which is easy to extract  
 381 gas molecules from ice effectively.  
 382  
 383

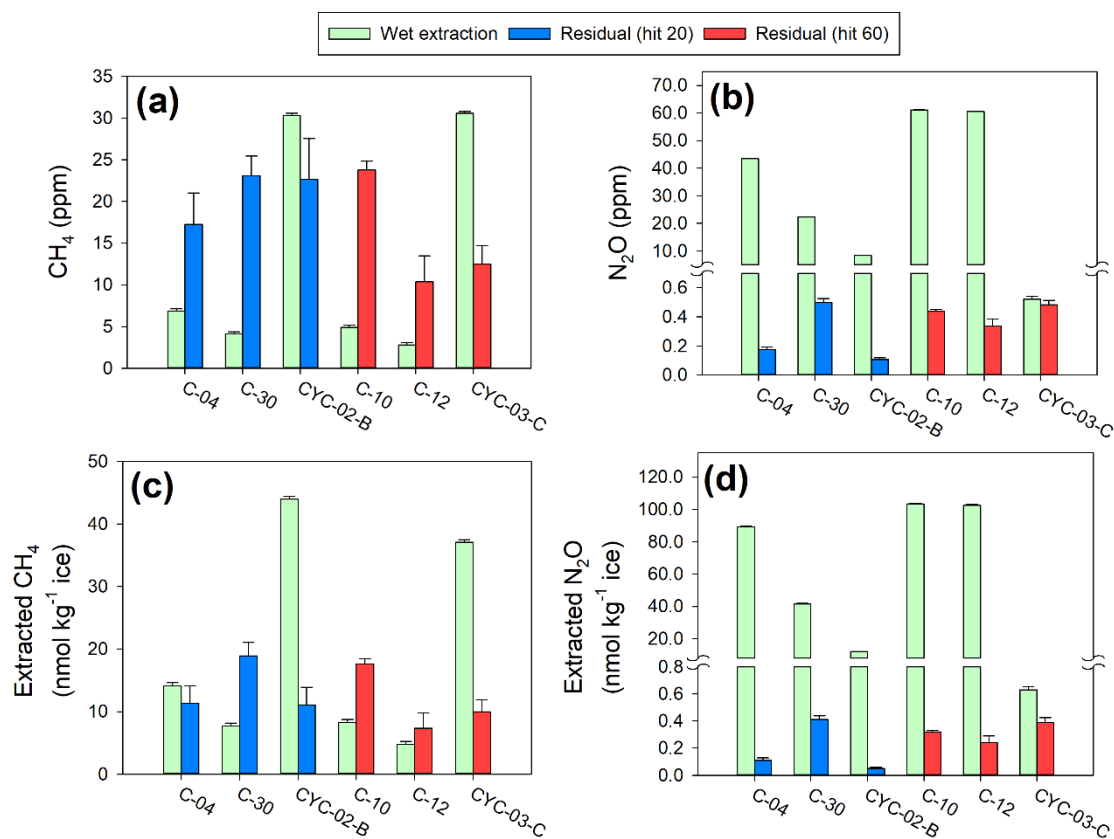


**Figure 2. Comparison of wet-extracted gas and residual gas for CH<sub>4</sub> and N<sub>2</sub>O mixing ratios (a and b) and contents (c and d).** The residual gas was extracted from the dry extraction method using the wet-degassed ice samples. The light green bars show the results of initial wet extraction, and the blue and red bars indicate the dry extraction of wet-degassed ice with 20- and 60-times hitting, respectively. The Cyuie samples are denoted as ‘CYC’, while ‘C’ indicates the Churapcha samples.

#### 384 4. Conclusions

385 In this study we carried out comparisons between wet and dry extractions, between  
386 untreated and biocide-treated wet extractions, and gas extraction from the easily to extract and  
387 difficult to extract parts of ice-wedge ice to better understand the characteristics of each  
388 extraction method, in order to adequately analyse CH<sub>4</sub> and N<sub>2</sub>O mixing ratios and gas contents  
389 from permafrost ice wedges. Based on these comparisons, our major findings are summarized  
390 as follows:

- 391 1) Existing wet and dry extraction methods allow gas extraction from the soft parts of  
392 ice (e.g., ice bubbles) and show insignificant differences in CH<sub>4</sub> and N<sub>2</sub>O mixing  
393 ratios.
- 394 2) Wet extraction results are unlikely to be affected by microbial production of CH<sub>4</sub>  
395 and N<sub>2</sub>O during the melting-refreeze procedure.
- 396 3) Both dry and wet extraction methods are not able to fully extract gas from ice wedge  
397 samples, presumably due to gas adsorbed on soil particles or enclosed within soil  
398 aggregates, which may have different gas mixing ratios compared to the gas in  
399 bubbles. Further research is required to develop a proper method to quantify and  
400 extract adsorbed and enclosed gases. In the meantime, we propose that both existing  
401 techniques may be suitable for gas mixing ratio measurements for bubbles in  
402 relatively soft ice wedges (i.e., easily crushed ice wedges by hit5 extraction, e.g.,  
403 Cyuie ice wedges in this study). Exceptionally, the N<sub>2</sub>O content in ice wedges may  
404 be measured by using repeated wet extractions, but this is not the case for  
405 determining the N<sub>2</sub>O mixing ratio.
- 406 4) Our findings indicate that previous estimates of ground ice CH<sub>4</sub> and N<sub>2</sub>O budget  
407 might be underestimated, implying that the greenhouse gas production in  
408 subfreezing environment of permafrost is larger than our current understanding.

409 5) Our finding indicates that the saturated NaCl solution is unnecessary to prevent  
410 microbial activity during melting, as employed by, e.g., Cherbunina et al. (2018).  
411 However, it remains as an open question how effectively the adsorbed gas  
412 molecules can be extracted by the method.

413

414

415 **Appendix. Systematic blank correction and uncertainty estimation**

416 Since the SNU dry extraction systems, including the sample tubes, were originally  
417 designed for CO<sub>2</sub> measurements from polar ice cores, these systems have not been tested for  
418 CH<sub>4</sub> and N<sub>2</sub>O analysis. We therefore carried out a series of tests to estimate the systematic  
419 blank, which is defined here as blanks.

420 The systematic blanks were tested with bubble-free ice (BFI) and standard air in a  
421 cylinder calibrated by NOAA. The BFIs were prepared as described in Yang et al. (2017). A  
422 major difference is that the BFI block was cut into small BFI pieces of 3–4 g, to mimic the  
423 random cube sampling protocol (see Materials and Methods section in the main text). The  
424 systematic blanks for the dry extraction method were tested as follows. A total of ~45 g of BFI  
425 cubes was placed into the crushing chamber, sealed with a copper gasket, and evacuated until  
426 the gas pressure inside the chamber dropped lower than ~60 mTorr, because of the vapor  
427 pressure formed by sublimation of the BFI. After evacuation was completed, standard gas was  
428 injected into the crushing chamber. The amount of standard injected was controlled by a  
429 volume calibrated vacuum line in the dry extraction system. Then the BFI samples were hit  
430 with the needle system 5 to 100 times, and the gases in the chamber were passed through a  
431 water trap and cryogenically pumped into the sample tubes, using the He-CCR. The number of  
432 hits did not significantly affect the systematic blank (Figure A2) and the regression curve for  
433 blank correction was fitted to the entire set of data points (red dashed curve in Figure A1).

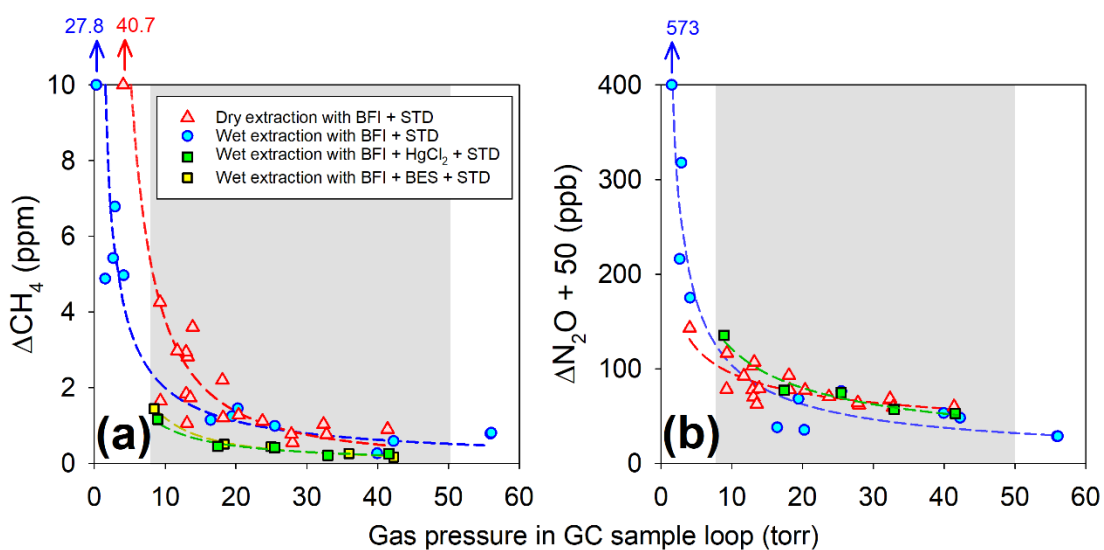
434 For the wet extraction, a total of ~45 g of BFI cubes was placed into each sample flask.  
435 The flasks were connected to the wet extraction line and sealed with a copper gasket, then  
436 evacuated. Once a vacuum was established, a known amount of standard gas was injected into  
437 each flask and the flasks were submerged into a warm water bath for ~40 min to melt  
438 completely. The flasks were then submerged into the cold ethanol bath, which was chilled to -  
439 80°C, to refreeze. For the HgCl<sub>2</sub> and Sodium 2-bromo-ethane-sulfonate (BES) treated

440 experiments, we first prepared the saturated solutions of  $\text{HgCl}_2$  and BES at room temperature  
441 ( $20^\circ\text{C}$ ) and added  $24\ \mu\text{L}$  of  $\text{HgCl}_2$  or  $20\ \mu\text{L}$  of BES solution into the empty flasks in a fume  
442 hood. Then we placed the flasks in a deep freezer, maintained at  $-45^\circ\text{C}$  for 20 min, to freeze  
443 the solutions before the BFI pieces were placed.

444 The results of the blank experiments are shown in Figure A1. The systematic blanks  
445 appear to be inversely correlated with the gas pressure in the sample tube. The systematic blank  
446 test results were fitted using exponential regression curves (dashed lines in Figure A1), and  
447 these regression curves were then used for systematic blank correction in our ice-wedge sample  
448 analyses.

449 To calculate uncertainties of the blank corrections, the blank test data were fitted with  
450 exponential regression curves (Figure A1). The root-mean-square-deviations (RMSD) of the  
451 data from the regression curves are taken as the uncertainties of blank corrections (Figure 1).  
452 Since the ice-wedge data used in this study showed the pressure in GC sample loop of about 8  
453  $\sim 50$  torr, the RMSD were estimated from the blank test data within this pressure range. The  
454 uncertainty of the gas content measurement is calculated by error propagation from those of  
455 pressure, line volume, and mass of ice samples.

456



457

**Figure A1.** Systematic blank of the needle crushing (dry extraction) and melting-refreezing (wet extraction) methods for (a)  $\text{CH}_4$  and (b)  $\text{N}_2\text{O}$  measurements in control and biocide ( $\text{HgCl}_2$ ) treated experiments. Also plotted are the  $\text{CH}_4$  blanks of BES-treated wet extractions. The dashed lines represent exponential regression curve fittings. Note that all data are plotted against the amount of gas trapped in the sample tube, presented here as the pressure in the GC sample loop when the sample gas is expanded. The grey shaded areas indicate the range of ice-wedge samples used in this study (see main text). The big-delta ( $\Delta$ ) notion in the y-axes indicate the offset from the values of the standard used.

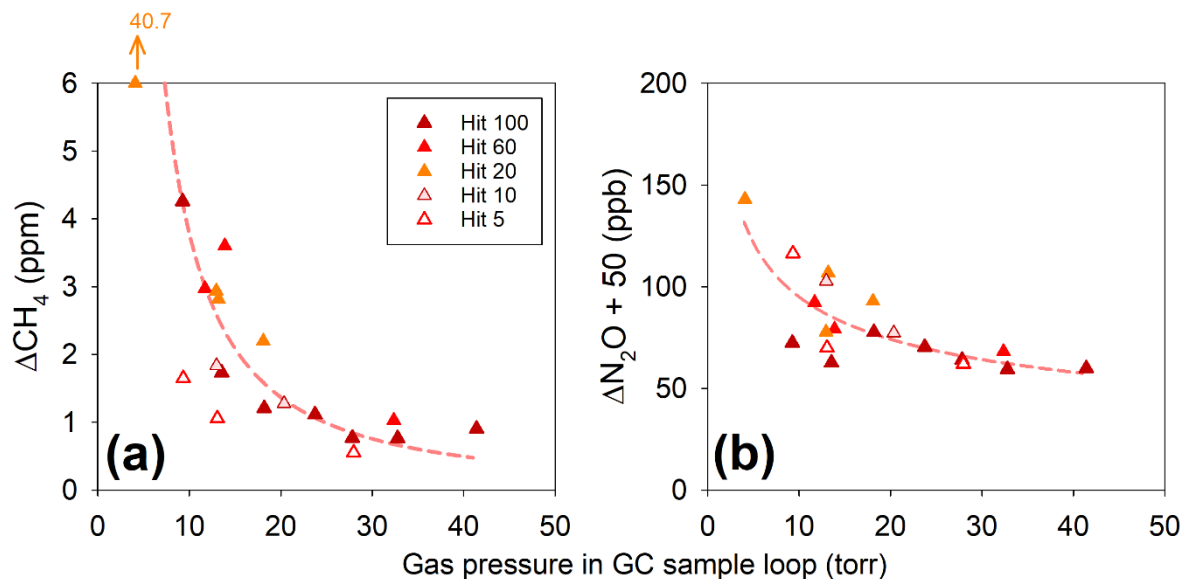


**Figure A2.** Influence of different number of hitting on the systematic blank of the needle crushing (dry extraction) system for (a)  $\text{CH}_4$  and (b)  $\text{N}_2\text{O}$  measurements. Note that all data are plotted against the amount of gas trapped in the sample tube, presented here as the pressure in the GC sample loop when the sample gas is expanded (see main text). The big-delta ( $\Delta$ ) notion in the y-axes indicate the offset from the values of the standard used.

458

459

460

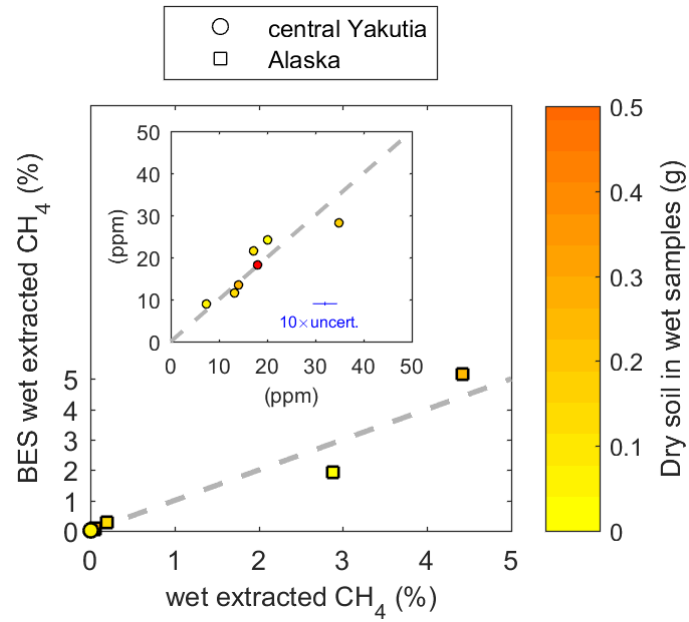


**Figure A3.** Comparison between control- and BES-treated wet extraction results for CH<sub>4</sub>. The sampling area is indicated by different symbols. The color of each data point indicates the dry soil weight in the subsamples used in control wet extraction. The grey dashed lines are 1:1 reference line. The blue error bar indicates the 1-sigma uncertainty of mixing ratios magnified by 10x.

461

462



463 **Table A1.** Comparison of results from extracted gas from the conventional wet extraction method and the residual gas in ice after 3-times wet extraction. The  
 464 residual gas was extracted by a needle crusher (see section 3.4 for details of the methods)

Site location	Sample	soil content	Wet extraction					Residual gas				
			gas content	CH <sub>4</sub> mixing ratio	N <sub>2</sub> O mixing ratio	CH <sub>4</sub> content	N <sub>2</sub> O content	gas content	CH <sub>4</sub> mixing ratio	N <sub>2</sub> O mixing ratio	CH <sub>4</sub> content	N <sub>2</sub> O content
		wt. %	ml/kg	ppm	ppm	nmol/kg	nmol/kg	ml/kg	ppm	ppm	nmol/kg	nmol/kg
Churapcha, central Yakutia	C-10	0.524	37.9	4.9	61.13	8.3	103	16.6	23.8	0.437	17.6	0.324
Churapcha, central Yakutia	C-30	1.03	41.7	4.1	22.28	7.7	41.5	18.4	23	0.50	19	0.41
Cyuie, central Yakutia	CYC-03-C	1.09	27.2	30.5	0.52	37.1	0.63	17.9	12.5	0.48	10.0	0.39
Churapcha, central Yakutia	C-04	1.38	46.0	6.9	43.46	14	89.2	14.7	17	0.17	11	0.11
Cyuie, central Yakutia	CYC-02-B	1.12	32.5	30.3	8.34	44.0	12.1	11.0	23	0.11	11	0.053
Churapcha, central Yakutia	C-12	0.370	38.0	2.8	60.47	4.8	103	15.9	10	0.34	7.3	0.24

465

466

467 **Data availability**

468 The data will be uploaded on the public data repository of Pangaea after publication.

469

470 **Author contributions**

471 JWY and JA conceived the research and designed the experiments. GI, JA, KK, and AF drilled the  
472 ice-wedge ice samples from Alaska and Siberia. JWY, JA, SH, and KK conducted the laboratory  
473 experiments. JWY and JA led the manuscript preparation with inputs from all other co-authors.

474

475 **Competing interests**

476 The authors declare no conflict interest.

477

478 **Acknowledgements**

479 The authors greatly acknowledge those who contributed to collect ice-wedge ice samples. We  
480 thank Gwangjin Lim and Jaeyoung Park for their help in sample preparations and gas extraction  
481 experiments, and Min Sub Sim for kind advice on inhibition experiment for methanogen.

482

483 **Financial support**

484 This project was supported by the Basic Science Research Program through the National Research  
485 Foundation of Korea (NRF) (NRF-2018R1A2B3003256 and NRF-2018R1A5A1024958) and the  
486 NASA ABoVE (Arctic Boreal and Vulnerability Experiment; grant no. NNX17AC57A).

487 **References**

- 488 Arkhangelov, A. A., and Novgorodova, E. V.: Genesis of massive ice at 'Ice Mountains', Yenesei  
489 River, Western Siberia, according to results of gas analyses, *Permafrost Periglac. Proc.*, 2,  
490 167-170, <http://doi.org/10.1002/ppp.3430020210>, 1991.
- 491 Bereiter, B., Stocker, T. F., and Fischer, H.: A centrifugal ice microtome for measurements of  
492 atmospheric CO<sub>2</sub> on air trapped in polar ice cores, *Atmos. Meas. Tech.*, 6, 251-262,  
493 <http://doi.org/10.5194/amt-6-251-2013>, 2013.
- 494 Boereboom, T., Samyn, D., Meyer, H., and Tison, J. -L.: Stable isotope and gas properties of two  
495 climatically contrasting (Pleistocene and Holocene) ice wedges from Cape Mamontov  
496 Klyk, Laptev Sea, northern Siberia, *The Cryosphere*, 7, 31-46, [http://doi.org/10.5194/tc-7-](http://doi.org/10.5194/tc-7-31-2013)  
497 [31-2013](http://doi.org/10.5194/tc-7-31-2013), 2013.
- 498 Brown, J., Ferrians Jr., O. J., Heginbottom, J. A., and Melnikov, E.: Circum-Arctic map of  
499 permafrost and ground-ice conditions, version 2, National Snow and Ice Data Center,  
500 Boulder, CO, 2002.
- 501 Cherbunina, M. Y., Shmelev, D. G., Brouchkov, A. V., Kazancev, V. S., and Argunov, R. N.:  
502 Patterns of spatial methane distribution in the upper layers of the permafrost in central  
503 Yakutia, *Mosc. Univ. Geol. Bull.*, 73, 100-108, 2018.
- 504 Fedorov, A. N., Botulu, T. A., Vasiliev, I. S., Varlamov, S. P., Gribanova, S. P., Dorofeev, I. V.:  
505 Permafrost-landscape map of the Yakut ASSR, Gosgeodezia, Moscow, Russia, Map, 1991  
506 (In Russian).
- 507 Higaki, S., Oya, Y., and Makide, Y.: Emission of methane from stainless steel surface investigated  
508 by using tritium as a radioactive tracer, *Chem. Lett.*, 35, 292-293,  
509 <https://doi.org/10.1246/cl.2006.292>, 2006.
- 510 Hugelius, G., Strauss, J., Zubrzycki, S., Harden, J. W., Schuur, E. A. G., Ping, C. -L., Schirrmeister,  
511 L., Grosse, G., Michaelson, G. J., Koven, C. D., O'Donnell, J. A., Elberling, B., Mishra,  
512 U., Camill, P., Yu, Z., Palmtag, J., and Kuhry, P.: Estimated stocks of circumpolar  
513 permafrost carbon with quantified uncertainty ranges and identified data gaps,  
514 *Biogeosciences*, 11, 6573-6593, <https://doi.org/10.5194/bg-11-6573-2014>, 2014.
- 515 Jorgenson, M. T., Kanevskiy, M., Shur Y, Moskalenko, N., Brown, D. R. N., Wickland, K., Striegl,  
516 R., and Koch, J.: Role of ground ice dynamics and ecological feedbacks in recent ice wedge

517 degradation and stabilization, *J. Geophys. Res.*, 120, 2280-2297,  
518 <https://doi.org/10.1002/2015JF003602>, 2015.

519 Kanevskiy, M., Shur, Y., Jorgenson, M. T., Ping, C. -L., Michaelson, G. J., Fortier, D., Stephani,  
520 E., Dillon, M., and Tums koy, V.: Ground ice in the upper permafrost of the Beaufort Sea  
521 coast of Alaska, *Cold Reg. Sci. Technol.*, 85, 56-70,  
522 <https://doi.org/10.1016/j.coldregions.2012.08.002>, 2013.

523 Katayama, T., Tanaka, M., Moriizumi, J., Nakamura, T., Brouchkov, A., Douglas, T. A., Fukuda,  
524 M., Tomita, F., and Asano, K.: Phylogenetic analysis of bacteria preserved in a permafrost  
525 ice wedge for 25,000 years, *Appl. Environ. Microbiol.*, 73, 2360-2363,  
526 <https://doi.org/10.1128/AEM.01715-06>, 2007.

527 Kim, K., Yang, J. -W., Yoon, H., Byun, E., Fedorov, A., Ryu, Y., and Ahn, J.: Greenhouse gas  
528 formation in ice wedges at Cuyie, central Yakutia, *Permafrost Periglac. Process.*, 30, 48-  
529 57, <http://doi.org/10.1002/ppp.1994>, 2019.

530 Lacelle, D., Radtke, K., Clark, I. D., Fisher, D., Lauriol, B., Utting, N., and Whyte, L. G.:  
531 Geomicrobiology and occluded O<sub>2</sub>-CO<sub>2</sub>-Ar gas analyses provide evidence of microbial  
532 respiration in ancient terrestrial ground ice, *Earth Planet. Sci. Lett.*, 306, 46-54,  
533 <https://doi.org/10.1016/j.epsl.2011.03.023>, 2011.

534 Masson-Delmotte, V., Schulz, M., Abe-Ouchi, A., Beer, J., Ganopolski, A., Rouco, J. F. G., Jansen,  
535 E., Lambeck, K., Luterbacher, J., Naish, T., Osborn, T., Otto-Bliesner, B., Quinn, T.,  
536 Ramesh, R., Rojas, M., Shao, X., and Timmerman, A.: Information from paleoclimatic  
537 archives, *Climate change 2013: The Physical science basis, Contribution of working group*  
538 *I to the fifth assessment report of the Intergovernmental Panel on Climate Change*, 383-  
539 464, <https://doi.org/10.1017/CBO9781107415324.013>, 2013.

540 Nollet, L., Demeyer, D., and Verstraete, W.: Effect of 2-bromoethanesulfonic acid and  
541 *Peptostreptococcus* products ATCC 35244 addition on stimulation of reductive  
542 acetogenesis in the ruminal ecosystem by selective inhibition of methanogenesis, *Appl.*  
543 *Environ. Microbiol.*, 63, 194-200, 1997.

544 Rivkina, E., Shcherbakova, V., Laurinavichius, K., Petrovskaya, L., Krivushin, K., Kraev, G.,  
545 Pecheritsina, S., and Gilichinsky, D.: Biogeochemistry of methane and methanogenic  
546 archaea in permafrost, *FEMS Microbiol. Ecol.*, 61, 1-15, [https://doi.org/10.1111/j.1574-](https://doi.org/10.1111/j.1574-6941.2007.00315.x)  
547 [6941.2007.00315.x](https://doi.org/10.1111/j.1574-6941.2007.00315.x), 2007.

548 Ryu, Y., Ahn, J., and Yang, J. -W.: High-precision measurement of N<sub>2</sub>O concentration in ice cores,  
549 Environ. Sci. Technol., 52, 731-738, <https://doi.org/10.1021/acs.est.7b05250>, 2018.

550 Salmon, V. G., Schadel, C., Bracho, R., Pegoraro, E., Celis, G., Mauritz, M., Mack, M. C., and  
551 Schuur, E. A. G.: Adding depth to our understanding of nitrogen dynamics in permafrost  
552 soils, J. Geophys. Res., 123, 2497-2512, <https://doi.org/10.1029/2018JG004518>, 2018.

553 Schaefer, H., Lourantou, A., Chappellaz, J., Luthi, D., Bereiter, B., and Barnola, J. -M.: On the  
554 stability of partially clathrated ice for analysis of concentration and  $\delta^{13}\text{C}$  of palaeo-  
555 atmospheric CO<sub>2</sub>, Earth Planet. Sci. Lett., 307, 334-340,  
556 <https://doi.org/10.1016/j.epsl.2011.05.007>, 2011.

557 Shin, J.: Atmospheric CO<sub>2</sub> variations on millennial time scales during the early Holocene, Master  
558 thesis, School of Earth and Environmental Sciences, Seoul National University, South  
559 Korea, 58 pp., 2014.

560 Strauss, J., Laboor, S., Fedorov, A. N., Fortier, D., Froese, D., Fuchs, M., Grosse, G., Günther, F.,  
561 Harden, J. W., Hugelius, G., Kanevskiy, M. Z., Kholodov, A. L., Kunitsky, V. V., Kraev, G.,  
562 Lapointe-Elmrabti, L., Lozhkin, A. V., Rivkina, E., Robinson, J., Schirrmeister, L.,  
563 Shmelev, D., Shur, Y., Siegert, C., Spektor, V., Ulrich, M., Vartanyan, S. L., Veremeeva, A.,  
564 Walter Anthony, K. M., and Zimov, S. A.: Database of Ice-Rich Yedoma Permafrost (IRYP),  
565 PANGAEA, <https://doi.org/10.1594/PANGAEA.861733>, 2016.

566 Torres, M. E., Mix, A. C., and Rugh, W. D.: Precise  $\delta^{13}\text{C}$  analysis of dissolved inorganic carbon in  
567 natural waters using automated headspace sampling and continuous-flow mass  
568 spectrometry, Limnol. Oceanogr.: Methods, 3, 349-360, 2005.

569 Yang, J. -W., Ahn, J., Brook, E. J., and Ryu, Y.: Atmospheric methane control mechanisms during  
570 the early Holocene, Clim. Past, 13, 1227-1242, <https://doi.org/10.5194/cp-13-1227-2017>,  
571 2017.

572 Yang, J. -W.: Paleoclimate reconstructions from greenhouse gas and borehole temperature of polar  
573 ice cores, and study on the origin of greenhouse gas in permafrost ice wedges, Ph.D. thesis,  
574 School of Earth and Environmental Sciences, Seoul National University, Seoul, 188 pp.,  
575 2019.

576